Scattering of focused electromagnetic waves by infinite cylinders

1969 J. Phys. A: Gen. Phys. 2 311

(http://iopscience.iop.org/0022-3689/2/3/010)

Scattering of focused electromagnetic waves by infinite cylinders

A. R. JONES
Department of Physics, Royal Holloway College, Egham, Surrey
MS. received 2nd *August* 1968, *in revised form* 9th *January* 1969

Abstract. The field near a line focus is developed in cylindrical coordinates, and the result is expressed in a series expansion readily applicable to scattering by an infinite cylinder. The properties of a line focus are found to be similar to those of a point focus. Scattering by metal cylinders is discussed, and it is shown that scattering of focused waves can be obtained by a simple modification of the existing theory for plane-wave scattering.

1. Introduction

Plasma diagnostics with microwaves is an established technique (Heald and Wharton 1965). However, the plasma often has dimensions of the same order as the microwave wavelength. In this case scattering is important, and leads to large errors if the infinite plane-slab approximation is used (Jones and Wooding 1967). If the plasma has a simple geometry the scattering problem can be solved rigorously, and a study of the scattered radiation can be used to measure the electron density (Jones and Wooding 1966).

An alternative is to reduce the incident beam width to be less than the plasma cross section, improving the infinite slab approximation. This has the added attraction of improved spatial resolution. The reduction in beam width may be achieved by the use of focusing lenses (Heald and Wharton 1965).

The Fresnel–Kirchhoff diffraction theory for the field near a point focus is well known (Born and Wolf 1964). Several authors have discussed the solution with emphasis on microwave lenses and the application to plasma diagnostics (Carswell and Richard 1964, Musil 1965).

Theory and experiment (Carswell and Richard 1964) show that the beam width near the focus is always finite. The minimum beam width obtainable is of the order of the wavelength. For plasmas of this size scattering is still significant. This paper examines this scattering for a line focus and infinite metal cylinders.

2. Theory of the line focus

The coordinate system used is shown in figure 1. The line focus is at the origin F. At the lens aperture the wave front is AA′, and by Huygens' principle each point Q on the wave front emits a spherical wave. The total effect at the point of observation P is the summation of these waves from all points on the wave front.

Assuming no variation with angle or z, the incident wave has the form

$$\psi_1 = \psi_0 S(\phi) \mathrm{H}_0^{(1)}(kr)$$

where $\mathrm{H}_0^{(1)}(kr)$ is a Hankel function of the first kind, $k = 2\pi/\lambda$ and $S(\phi)$ is the field distribution on the lens aperture. For uniform illumination of the lens aperture we choose $S(\phi) = 1$.

The cylindrical wave generated at the point Q is

$$\psi_2 = \mathrm{i}\pi \mathrm{H}_0^{(2)}(kr)$$

which is the appropriate Green function of the scalar Helmholtz equation (Morse and Feshbach 1953). The Fresnel–Kirchhoff integral is thus

$$\psi_{\mathrm{P}} = \frac{f}{4\pi} \int_{\phi} \left(\psi_2 \frac{\partial \psi_1}{\partial n} - \psi_1 \frac{\partial \psi_2}{\partial n} \right) \mathrm{d}\phi \tag{1}$$

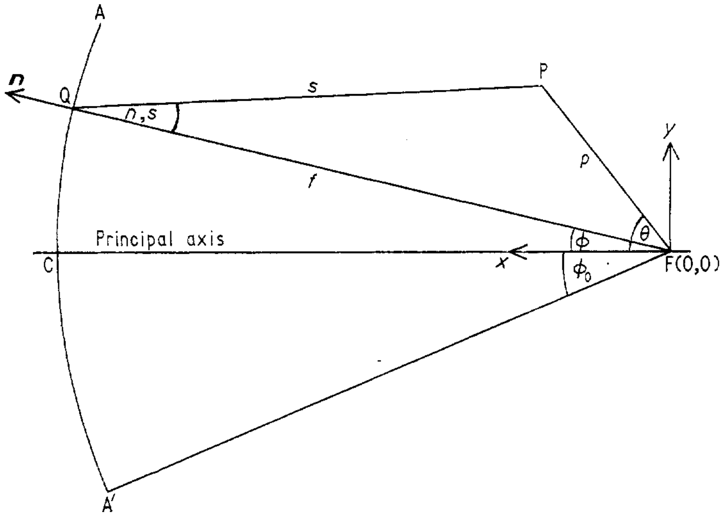

Figure 1. Coordinate system for the line focus.

where $\boldsymbol{n}$ is a unit vector normal to the wave front. Now

$$\frac{\partial\psi_1}{\partial n} = \psi_0 k \frac{\mathrm{dH}_0^{(1)}(kr)}{\mathrm{d}(kr)}\bigg|_{r=f} = -\psi_0 k \mathrm{H}_1^{(1)}(kf).$$

Also

$$\frac{\partial\psi_2}{\partial n} = \mathrm{i}\pi k \frac{\mathrm{dH}_0^{(2)}(kr)}{\mathrm{d}(kr)}\bigg|_{r=s} \cos(n,s) = -\mathrm{i}\pi k \mathrm{H}_1^{(2)}(ks)\cos(n,s).$$

Equation (1) becomes

$$\psi_{\mathrm{P}} = \frac{\mathrm{i}\psi_0 kf}{4}\int_\phi \{\mathrm{H}_0^{(1)}(kf)\mathrm{H}_1^{(2)}(ks)\cos(n,s) - \mathrm{H}_1^{(1)}(kf)\mathrm{H}_0^{(2)}(ks)\}\,\mathrm{d}\phi. \quad (2)$$

For points near the focus $\rho/f \ll 1$, so that

$$s \simeq f\left\{1 - \frac{\rho}{f}\cos(\theta-\phi)\right\}$$

and

$$\frac{1}{s^{n/2}} \simeq \frac{1}{f^{n/2}}\left\{1 + \frac{n\rho}{2f}\cos(\theta-\phi)\right\}.$$

Using these approximations

$$\cos(n,s) = \frac{s^2+f^2-\rho^2}{2sf} \simeq 1 - \frac{\rho^2}{f^2}\cos^2(\theta-\phi)$$

or

$$\cos(n,s) \simeq 1.$$

Using the approximations for $|kr| \gg 1$

$$\mathrm{H}_n^{(1)}(kr) \simeq \left(\frac{2}{\pi kr}\right)^{1/2} \exp\{\mathrm{i}(kr - \tfrac{1}{2}n\pi - \tfrac{1}{4}\pi)\}$$

$$\mathrm{H}_n^{(2)}(kr) = \left(\frac{2}{\pi kr}\right)^{1/2} \exp\{-\mathrm{i}(kr - \tfrac{1}{2}n\pi - \tfrac{1}{4}\pi)\}$$

equation (2) now reduces to

$$\psi_P = -\frac{\psi_0}{\pi}\int_\phi \left\{1+\frac{\rho}{2f}\cos(\theta-\phi)\right\}\exp\{ik\rho\cos(\theta-\phi)\}\,d\phi. \tag{3}$$

To evaluate the integral we use Neumann's expansion

$$\exp\{ik\rho\cos(\theta-\phi)\} = \sum_{n=-\infty}^{\infty} i^n J_n(k\rho)\cos\{n(\theta-\phi)\}$$

where $J_n(k\rho)$ is a Bessel function, and n an integer.

2.1. *Approximation with* $\rho/f \ll 1$

The integral in equation (3) becomes

$$\psi_P = -\frac{\psi_0}{\pi}\int_{-\phi_0}^{\phi_0}\exp\{ik\rho\cos(\theta-\phi)\}\,d\phi$$

where ϕ_0 is the angle subtended by half the lens aperture at the focus. Use of Neumann's expansion and integration term by term gives

$$\psi_P = -\frac{2\psi_0}{\pi}\sum_{n=-\infty}^{\infty} i^n J_n(k\rho)\frac{\sin n\phi_0}{n}\cos n\theta \tag{4}$$

2.2. *The complete integral*

The second term in equation (3) was

$$\Delta\psi_P = -\frac{\psi_0}{\pi}\frac{\rho}{2f}\int_{-\phi_0}^{\phi_0}\cos(\theta-\phi)\exp\{ik\rho\cos(\theta-\phi)\}\,d\phi.$$

Again using Neumann's expansion and integrating term by term we have

$$\Delta\psi_P = -\frac{\psi_0}{\pi}\frac{\rho}{2f}\sum_{n=-\infty}^{\infty} i^n J_n(k\rho)\left\{\frac{\sin(n+1)\phi_0}{n+1}\cos(n+1)\theta + \frac{\sin(n-1)\phi_0}{n-1}\cos(n-1)\theta\right\}. \tag{5}$$

Combining equations (4) and (5), and using the symmetry of terms in n, we have for the complete solution

$$\psi_P = -2\frac{\psi_0}{\pi}\sum_{n=0}^{\infty}\epsilon_n i^n J_n(k\rho)\left[\frac{\sin n\phi_0}{n}\cos n\theta + \frac{\rho}{4f}\left\{\frac{\sin(n+1)\phi_0}{n+1}\cos(n+1)\theta+\frac{\sin(n-1)\phi_0}{n-1}\cos(n-1)\theta\right\}\right] \tag{6}$$

where $\epsilon_0 = 1$, $\epsilon_n = 2$ $(n \neq 0)$.

3. Properties of the line focus

Calculations of equation (6) were performed on the University of London Atlas computer, using FORTRAN V. For $f/\lambda = 10$, $kf \sim 60$ and $30 \lesssim ks \lesssim 90$. In this region the use of the asymptotic approximation for the Bessel functions introduces an error of less than 5%. The effect of the term $\Delta\psi_P$ is illustrated in figure 2. When the term is included the maximum along the axis occurs not at the focus but between the focus and the lens, as seen in figure 2(*a*). For $|\rho/f| = \frac{1}{2}$, $\Delta\psi_P$ is 6% of ψ_P. Figure 2(*b*) shows the variation of phase in the transverse focal plane. There is a phase change of 180° between adjacent

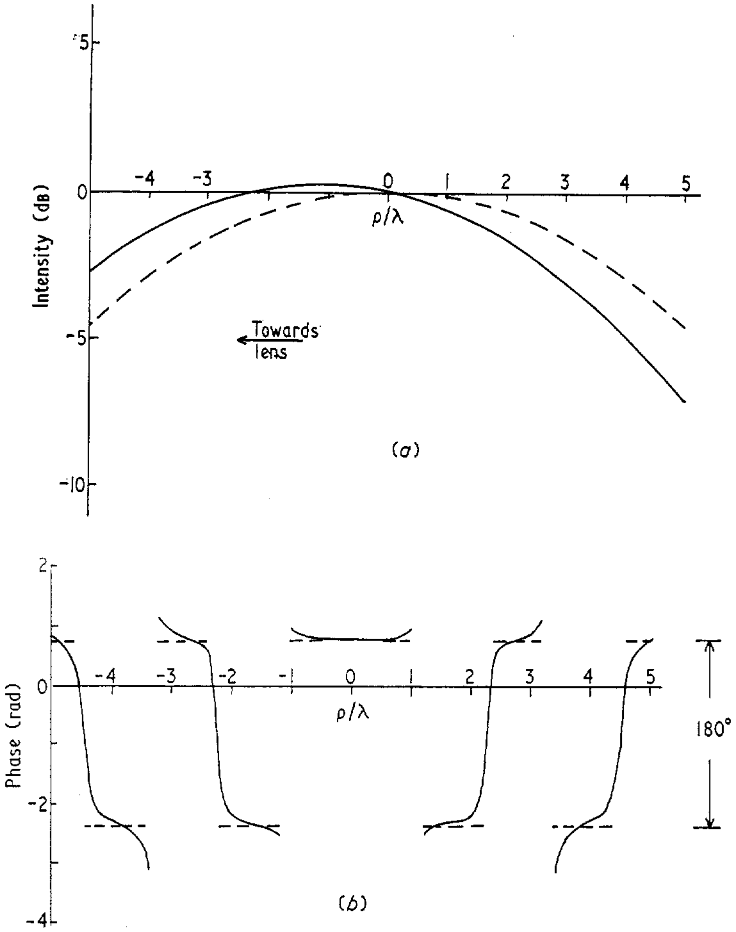

Figure 2. Effect of the term $\Delta\psi_P$ ($f/\lambda = 10$, $D/\lambda = 10$): (*a*) intensity variation along the principal axis; (*b*) phase variation in the transverse focal plane. Full curve, including $\Delta\psi_P$; broken curve, excluding $\Delta\psi_P$.

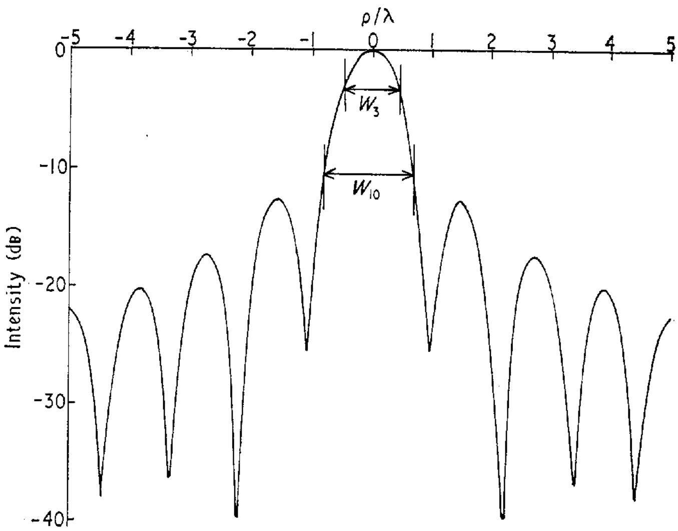

Figure 3. Intensity variation in the transverse focal plane ($f/\lambda = 10$, $D/\lambda = 10$).

maxima in the intensity. Equation (4) alone produces a discontinuous step, but inclusion of $\Delta\psi_P$ shows a smooth transition. Because of its evident importance the term $\Delta\psi_P$ is included in all the following results. The next term in the series is $O(\rho^2/f^2)$ and should contribute less than $\frac{1}{2}\%$. It is not considered here.

A typical example of the intensity variation in the transverse focal plane ($\theta = 90°$ and $\theta = 270°$) is shown in figure 3. The spatial resolution depends upon the width of the central peak. Two widths are defined at -3 dB (W_3) and at -10 dB (W_{10}) as shown. The width is seen in figure 4 to be a function of f number (F_{n0}) only, where $F_{n0} = f/D$. The width is always finite.

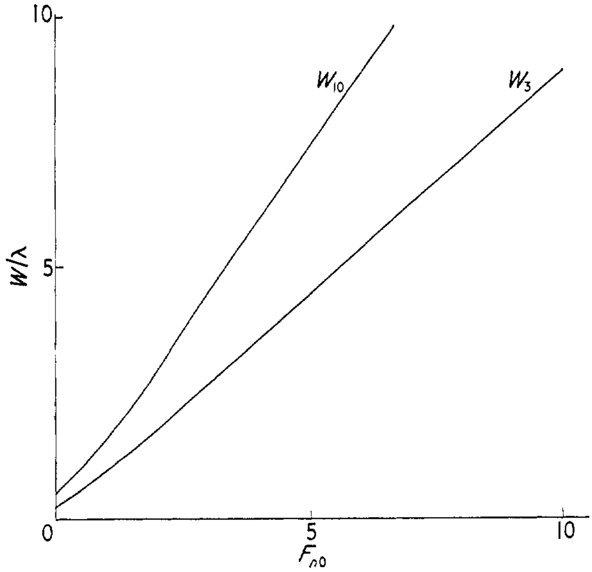

Figure 4. Beam width as a function of f number.

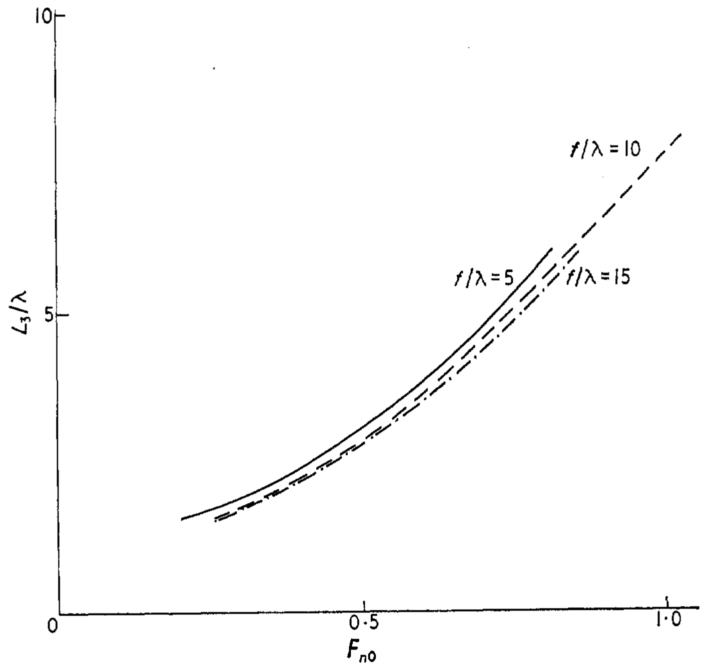

Figure 5. Beam length as a function of f number.

Strictly the scalar diffraction theory is valid only for $f \gg D \gg \lambda$ and $f \gg \rho$. The first of these conditions is certainly not satisfied here since $f \leqslant D$ is used, and the other conditions are only marginally satisfied because of the long wavelength. However, the experimental results of Richard (1968) indicate a remarkable agreement with theory, to within 30% at $f_{n0} = 0{\cdot}38$. Thus the scalar theory is expected to show the correct features to within 50%.

The central maximum along the principal axis is between the focus and the lens, and approaches the focus as the aperture is increased. The length of the central peak decreases with increasing aperture. The length at -3 dB of the maximum (L_3) is shown in figure 5. There is some dependence upon the focal length. Again the length is always finite.

The phase variation along the principal axis is cyclic. A 'guide wavelength' λ_g may be defined as the distance separating points of equal phase, and is found to be greater than the free-space wavelength. This is shown as a function of F_{n0} in figure 6.

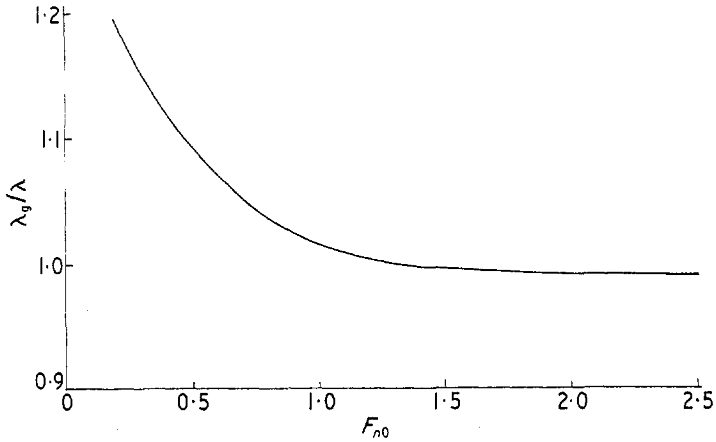

Figure 6. Variation of 'guide wavelength' λ_g with f number.

The results outlined above show that a line focus has similar properties to a point focus, but in two dimensions.

4. Theory of scattering of a focused beam by a metal cylinder

The incident field is described by equation (6). Two cases are considered: (*a*) parallel polarization ($E_{\parallel}$), the electric vector being parallel to the cylinder axis, and (*b*) perpendicular polarization ($E_{\perp}$) with the magnetic vector parallel to the cylinder axis.

4.1. *Parallel polarization* ($E_{\parallel}$)

The incident electric field E_z^{I} is described by equation (6). If E_z^{S} is the scattered electric field the boundary condition at the surface of the cylinder ($\rho = a$) is

$$E_z^{\mathrm{I}} + E_z^{\mathrm{S}} = 0. \tag{7}$$

The scattered field is a cylindrical wave of the form

$$E_z^{\mathrm{S}} = \sum_{n=0}^{\infty} A_n \mathrm{H}_n^{(1)}(k\rho) \cos n\theta. \tag{8}$$

Multiplying both sides of equation (7) by $\cos n\theta \, \mathrm{d}\theta$ and integrating from $-\pi$ to π we have

$$-A_n \mathrm{H}_n^{(1)}(ka) = -2\frac{\psi_0}{\pi}\epsilon_n \mathrm{i}^n \frac{\sin n\phi_0}{n}\left[\mathrm{J}_n(ka) - \frac{\mathrm{i}a}{2f}\{\mathrm{J}_{n-1}(ka) - \mathrm{J}_{n+1}(ka)\}\right].$$

Use of the recurrence relation for Bessel functions reduces this to

$$A_n = \frac{2\psi_0}{\pi}\epsilon_n \mathrm{i}^n \frac{\sin n\phi_0}{n}\frac{\mathrm{J}_n(ka) - \mathrm{i}(a/2f)\mathrm{J}_n'(ka)}{\mathrm{H}_n^{(1)}(ka)}. \tag{9}$$

Thus the theory is the same as that for plane-wave scattering except that

$$\mathrm{J}_n(ka) \to -\frac{2\psi_0}{\pi}\frac{\sin n\phi_0}{n}\left\{\mathrm{J}_n(ka) - \frac{\mathrm{i}a}{2f}\mathrm{J}_n'(ka)\right\}. \tag{10}$$

4.2. *Perpendicular polarization* ($E_\perp$)

The incident magnetic field H_z^{I} is described by equation (6). The boundary condition at $\rho = a$ is

$$E_\theta^{\mathrm{I}} + E_\theta^{\mathrm{S}} = 0 \tag{11}$$

where from Maxwell's equations

$$E_\theta = \frac{\mathrm{i}}{k}\frac{\partial H_z}{\partial \rho}.$$

The scattered magnetic field is

$$H_z^{\mathrm{S}} = \sum_{n=0}^{\infty} B_n H_n^{(1)}(k\rho)\cos n\theta. \tag{12}$$

Multiplying both sides of equation (11) by $\cos n\theta \, \mathrm{d}\theta$ and integrating from $-\pi$ to π we have

$$-B_n \mathrm{H}_n^{(1)\prime}(ka) = -\frac{2\psi_0}{\pi}\epsilon_n \mathrm{i}^n \left(\frac{\sin n\phi_0}{n}\left[\mathrm{J}_n'(ka) - \frac{\mathrm{i}a}{4f}\{\mathrm{J}'_{n-1}(ka) - \mathrm{J}'_{n+1}(ka)\}\right] - \frac{\sin n\phi_0}{n}\frac{\mathrm{i}}{4kf}\{\mathrm{J}_{n-1}(ka) - \mathrm{J}_{n+1}(ka)\}\right).$$

Use of the recurrence relations for Bessel functions reduces this to

$$B_n = \frac{2\psi_0}{\pi}\epsilon_n \mathrm{i}^n \frac{\sin n\phi_0}{n}\frac{\mathrm{J}_n'(ka)(1 - \mathrm{i}/2kf) - (\mathrm{i}a/2f)\mathrm{J}_n''(ka)}{\mathrm{H}_n^{(1)\prime}(ka)}. \tag{13}$$

The prime denotes differentiation with respect to the argument.

Again this theory is the same as that for plane-wave scattering except that

$$\mathrm{J}_n'(ka) \to -\frac{2\psi_0}{\pi}\frac{\sin n\phi_0}{n}\left\{\mathrm{J}_n'(ka)\left(1 - \frac{\mathrm{i}}{2kf}\right) - \frac{\mathrm{i}a}{2f}\mathrm{J}_n''(ka)\right\}. \tag{14}$$

This theory may be applied directly to scattering by dielectric cylinders. The only requirement is that the Bessel functions describing the incident plane wave be replaced by the appropriate function in equations (10) or (14).

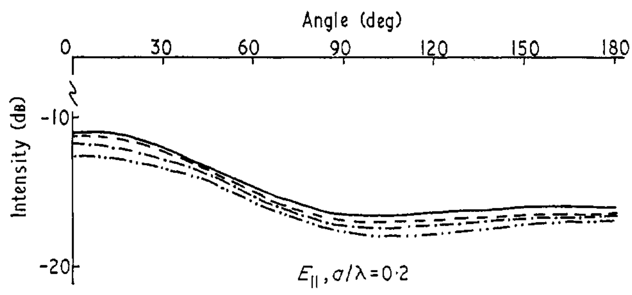

Figure 7(*a*).

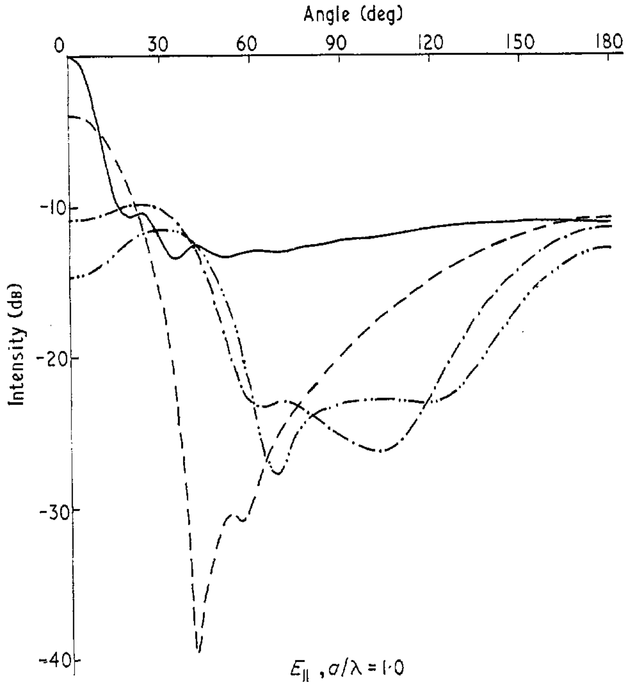

Figure 7(*b*).

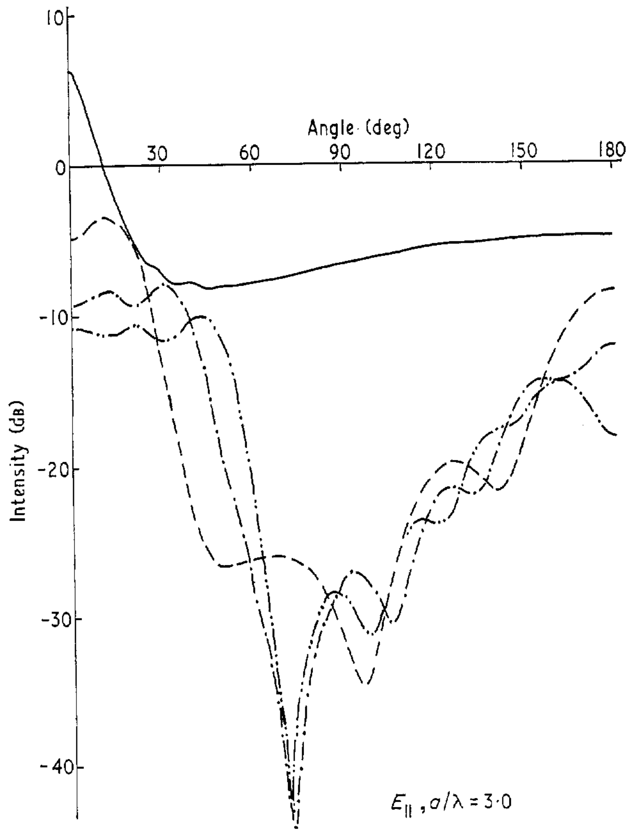

Figure 7(*c*).

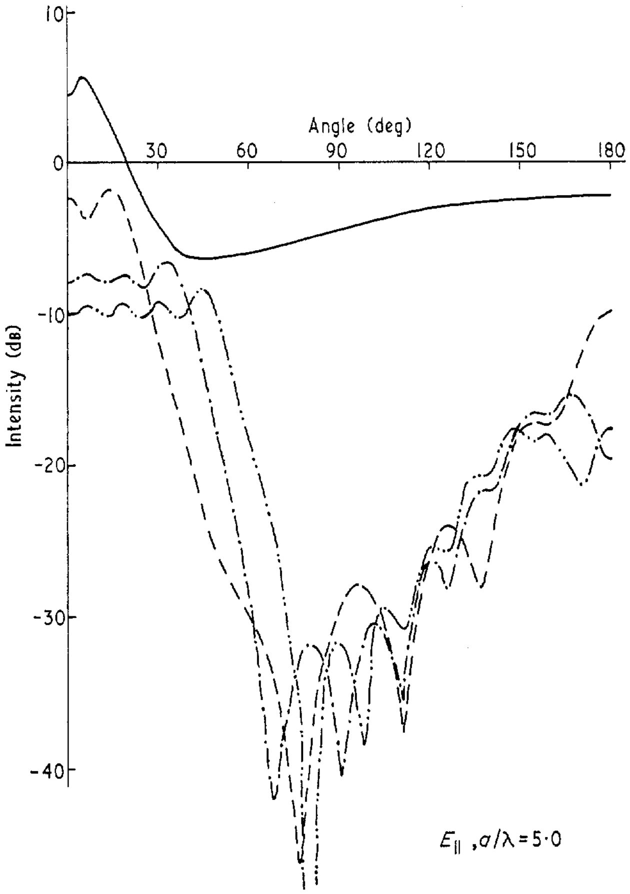

Figure 7(*d*).

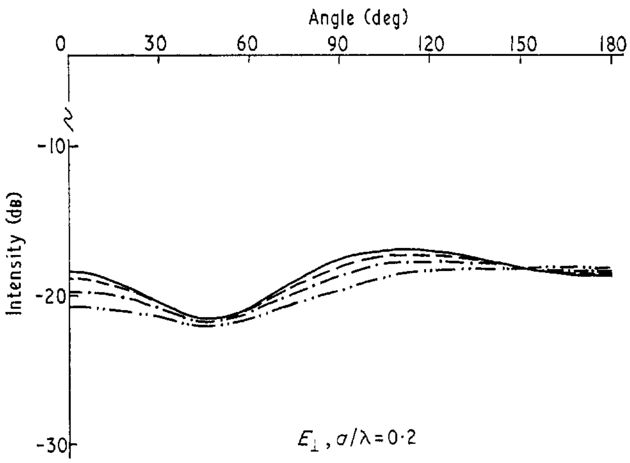

Figure 7(*e*).

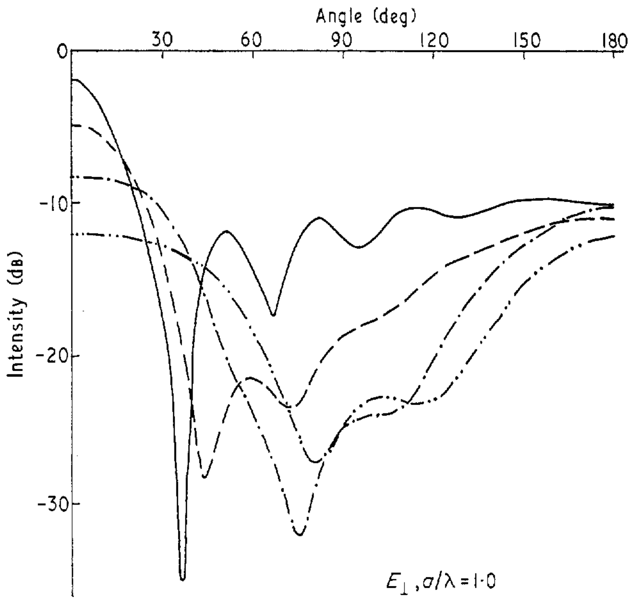

Figure 7(f).

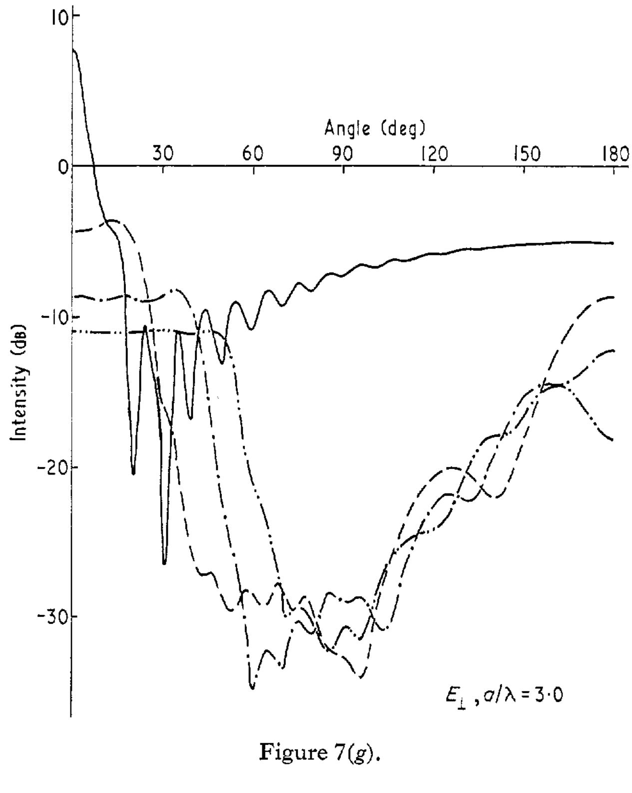

Figure 7(g).

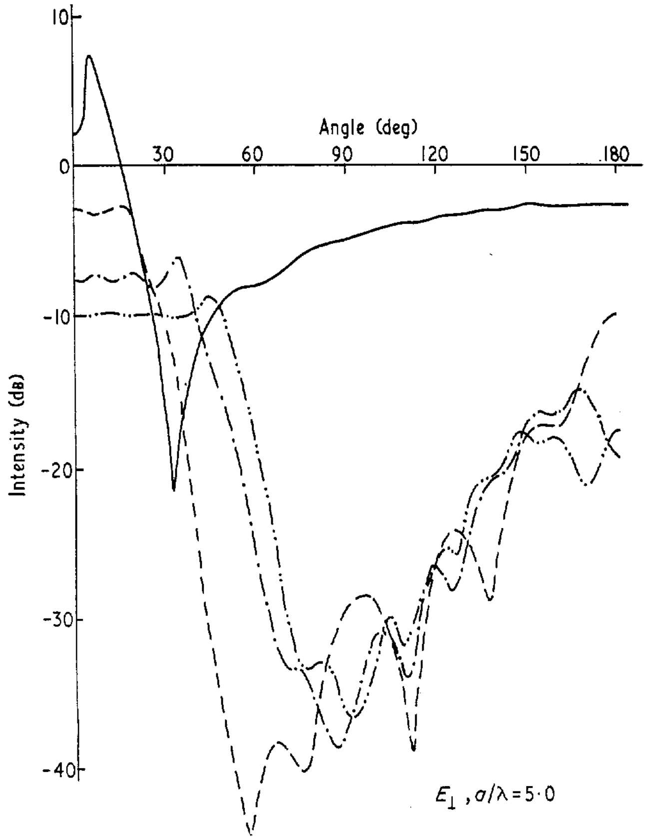

Figure 7(*h*).

Figure 7(*a*)–(*h*). Scattering of a line focused wave by metal cylinders ($kR = 100$). ——— plane wave; – – – focused wave ($f/\lambda = 10$, $F_{n0} = 1 \cdot 0$); –·–·– focused wave ($f/\lambda = 10$, $F_{n0} = 0 \cdot 5$); —··——··— focused wave ($f/\lambda = 10$, $F_{n0} = 0 \cdot 3$).

5. Computed scattering of a focused wave by a metal cylinder

Computations were performed for both polarizations for plane-wave and focused-wave scattering. The results are presented in figure 7 for a range of a/λ and f number. The detector is taken at a radius R such that $kR = 100$. This number was chosen for convenience.

All the curves are drawn to the same scale for ready comparison. The intensities are normalized in two ways: first relative to the intensity at the origin (this is unity for a plane wave), and second relative to the forward scattered intensity with parallel polarization ($E_{\parallel}$, $\theta = 0°$) of a plane wave by a cylinder of radius $a/\lambda = 1 \cdot 0$.

In the immediate vicinity of the focus the focused waves are approximately plane. For a very small cylinder the scattering by focused and plane waves should be similar. This is shown to be true for $a/\lambda = 0 \cdot 2$ in figures 7(*a*) and 7(*e*).

For the larger cylinders ($a/\lambda \geqslant 1 \cdot 5$) there is very little scattering perpendicular to the direction of incidence of a focused wave compared with plane-wave scattering. This is expected from the plane-slab approximation, where all the incident power should be reflected into $\theta = 180°$.

The scattered intensity shows two major peaks. There is the large peak of reflected intensity ($\theta = 180°$) and a large peak in the forward direction ($\theta = 0°$). But there should be a shadow in the forward direction, and it is important to note that this peak is of scattered intensity. To obtain the shadow the diffraction pattern would have to be determined. The diffracted field E_z^{D} is given by (van der Hulst 1957)

$$E_z^{\mathrm{D}} = E_z^{\mathrm{I}} + E_z^{\mathrm{S}}.$$

For a plane wave the reflected intensity increases monotonically with cylinder radius. However, this is not true for focused waves, the reflected intensity reaching a peak and then decreasing. Further, the intensity reflected by the larger cylinders is less for the smaller f numbers, and therefore narrower beams. This is opposite to what would be predicted by an improved slab approximation.

It is suggested that both these properties are due to the finite size of the beam in the focal region. As the cylinder radius increases the field strength at the cylinder surface decreases, and decreases more rapidly for the smaller f numbers.

6. Conclusion

The electromagnetic field in the vicinity of a line focus has been expressed in cylindrical coordinates, and an expansion obtained in a form readily applicable to cylindrical scattering problems. The line focus has been shown to have properties similar to those of a point focus (Carswell and Richard 1964).

The scattering by an infinite cylinder of a line focused wave can be obtained by a simple modification of the existing theory for scattering of a plane wave. An infinite plane metal slab for normal incidence would show a large reflected signal only and nothing perpendicular to the incident beam. Scattering of a focused wave by cylinders of moderate size ($a/\lambda \geqslant 1{\cdot}5$) exhibits similar properties.

Carswell and Richard (1964) pointed out that the ideal beam shape for plasma diagnostics would be long and narrow. However, the beam length and beam width decrease together, a consequence of which is the anomalous behaviour of the reflected signal. The infinite plane slab approximation cannot readily be used.

The study of scattering of a focused beam overcomes this difficulty. The improved spatial resolution is retained, and the possibility arises of studying inhomogeneities by focusing the beam at different points within a plasma. For this purpose the energy should be concentrated into as small a volume as possible, requiring lenses of very large aperture.

The scalar theory as outlined here provides only an estimate of the effects of a focused beam on scattering. At microwave wavelengths the full vector theory must be used to obtain a rigorous result.

Acknowledgments

The author is grateful to Professor S. Tolansky and the Royal Holloway College for providing facilities for this work.

References

Born, M., and Wolf, E., 1964, *Principles of Optics*, 2nd edn (Oxford: Pergamon Press).

Carswell, A. I., and Richard, C., 1964, *RCA Victor Res. Rep.*, No. 7-801-32.

Heald, M. A., and Wharton, C. B., 1965, *Plasma Diagnostics with Microwaves* (New York: John Wiley).

van der Hulst, H. C., 1957, *Light Scattering by Small Particles* (London: Chapman and Hall).

Jones, A. R., and Wooding, E. R., 1966, *J. Appl. Phys.*, **37**, 4670–6.

—— 1967, *Plasma Phys.*, **9**, 737–40.

Morse, P. M., and Feshbach, H., 1953, *Methods of Theoretical Physics* (New York: McGraw-Hill), p. 811.

Musil, J., 1965, *Res. Rep. Czech. Acad. Sci.*, No. IPPCZ-51.

Richard, C., 1968, *RCA Victor Res. Rep.*, No. 3-900-11.